



CERN-PBC-NOTE 2023-002

7 March 2023

Jamie.Boyd@cern.ch

## Update on the FPF Facility technical studies

FPF PBC Working Group:

M. Andreini, G. Arduini, K. Balazs, J. Boyd, R. Bozzi, F. Cerutti, F. Corsanego, J-P. Corso, L. Elie, A. Infantino, A. Navascues Cornago, J. Osborne, G. Peon, M. Sabaté Gilarte  
CERN, CH-1211 Geneva, Switzerland

Keywords: FPF

---

---

### Summary

The Forward Physics Facility (FPF) is a proposed new facility to house several new experiments at the CERN High Luminosity LHC (HL-LHC). The FPF is located such that the experiments can be aligned with the collision axis line of sight (LOS), a location which allows many interesting physics measurements and searches for new physics to be carried out. The status of technical studies related to the FPF, as well as the physics potential were documented in Ref. [1] which was released in March 2022. This note documents updates to the FPF technical studies completed since that time.

---

# Contents

<b>1</b>	<b>Introduction</b>	<b>3</b>
<b>2</b>	<b>Civil Engineering Design Update</b>	<b>4</b>
2.1	Safety Gallery . . . . .	4
2.2	Roads and networks . . . . .	4
2.3	Proposed Site Investigation Works . . . . .	5
<b>3</b>	<b>Ventilation System</b>	<b>7</b>
<b>4</b>	<b>Background particle rates at the FPF</b>	<b>9</b>
4.1	Simulation technique . . . . .	9
4.2	Effect of full magnetic field maps of Long Straight Section magnets . . . . .	9
4.3	Sweeper magnet potential . . . . .	10
4.4	First estimation of neutron field . . . . .	13
<b>5</b>	<b>Radiation Protection studies</b>	<b>15</b>
<b>6</b>	<b>Summary</b>	<b>24</b>

# 1 Introduction

The Forward Physics Facility (FPF) is a proposed new facility to house several experiments in the very forward region of the IP1 LHC collisions during the HL-LHC. Technical studies related to the FPF have been carried out in the context of a dedicated working group as part of the CERN Physics Beyond Colliders (PBC) Study Group [2]. At the same time many physics sensitivity studies have been carried out, highlighting the broad and deep physics case for the proposed experiments at the FPF. The physics case covers searches for light, weakly coupled dark sector particles, studies of large samples of high energy neutrinos of all flavours and QCD measurements from probing very forward hadron production and deep inelastic scattering experiments with high energy neutrinos.

A detailed write up of the FPF status as a White paper for the US Snowmass process was released in March 2022 [1]. Since then, technical studies related to the FPF have continued, leading to some changes in the facility design, and some more mature results related to the expected particle background rates, and radiation levels in the cavern. This note documents the results and conclusions from the updated technical studies.

## 2 Civil Engineering Design Update

### 2.1 Safety Gallery

The version of the FPF facility design described in Ref. [1], had a safety corridor connecting the FPF cavern to the LHC tunnel, with the idea this could be used as an escape route in case of a fire or other safety incident that blocked escape via the FPF shaft. However, the connection to the LHC introduced a number of potential issues related to the structural safety of the LHC tunnel, and heavily constrained the possible timeline when the FPF could be implemented. After further discussions with the CERN safety group it was concluded that the connection to the LHC could be dropped, and instead a pressurized safety corridor was proposed along the side of the cavern, to allow evacuation in case of a fire blocking the main route. Figure 1 shows the updated layout of the underground facility.

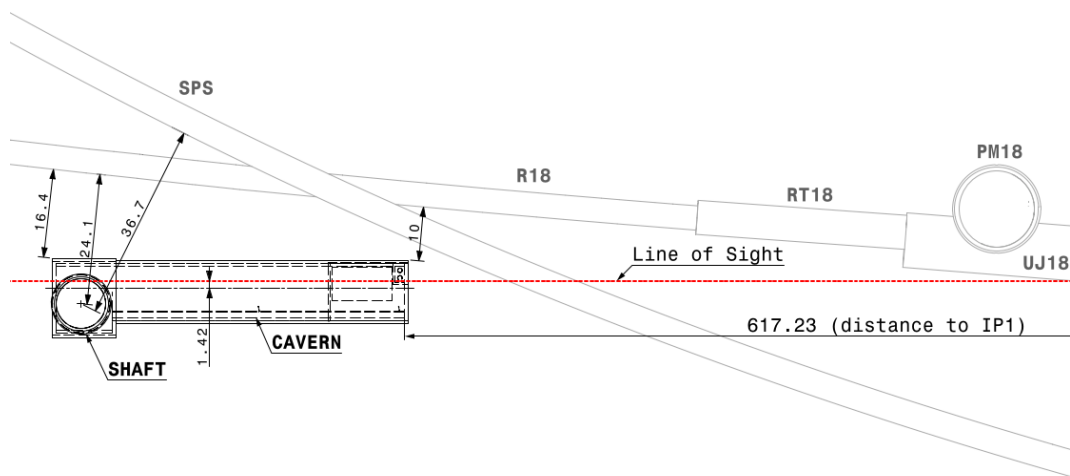


Figure 1: Situation plan of the underground facility with the proposed safety corridor inside the cavern

To accommodate the proposed 1.2m wide corridor while leaving enough space around the experiments the width of the cavern was increased from 8.5 m to 9.6 m. The location of the access lift and stairs was also modified to be directly connected to the corridor thus creating a safe evacuation path in case of an accident.

The corridor will be accessible from the inside of the cavern through two fire resistant doors, one located at the far end of the cavern and the other at the middle allowing a safe evacuation to the pressurised area at the bottom of the shaft as shown in the Figure 2 and Figure 3.

### 2.2 Roads and networks

Previously the proposed layout of the FPF surface area included an access road linking the new surface buildings to the existing roads and infrastructure of the SM18 buildings at the northeast.

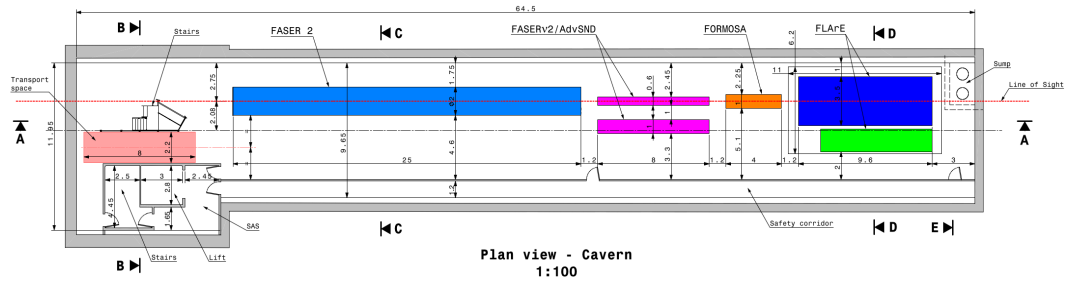


Figure 2: General layout of the FPF cavern and the access shaft. The coloured boxes indicate the possible experiments.

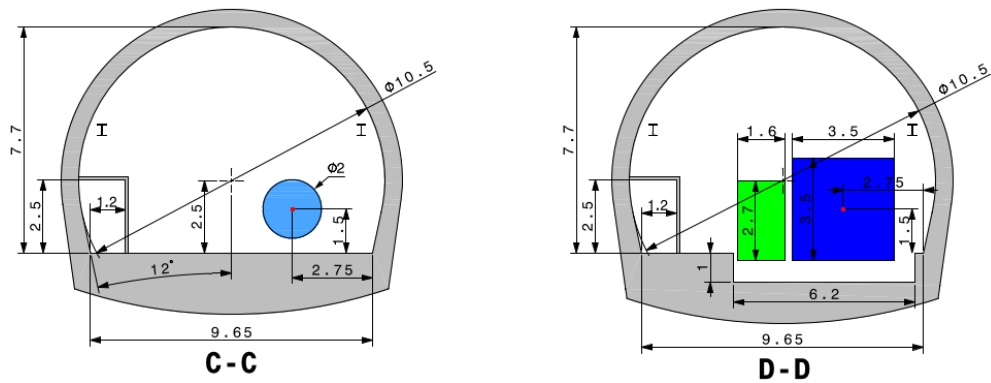


Figure 3: Cross sections through the cavern and safety corridor. Section C-C shows the FASER2 detector, and section D-D shows the FLArE detector in blue, a possible cooling unit in green and a 1 m-deep trench.

Following a detailed study of the existing service networks in the area a new design of the surface buildings and the surrounding area has been developed to avoid interferences with the existing networks. In this configuration the access to the FPF site will be from the east, close to the SHM18 building (Bldg. 3177) and the two auxiliary buildings are proposed on the other side of the access building avoiding any possible interference with the existing networks as shown in the Figure 4.

### 2.3 Proposed Site Investigation Works

A preliminary site investigation is planned to be carried out early in 2023 when a new single core will be drilled to the full depth of the proposed shaft. As part of the study a soil investigation interpretation report will be prepared providing commentary and advice on impacts for the execution of the Civil Engineering (CE) works.

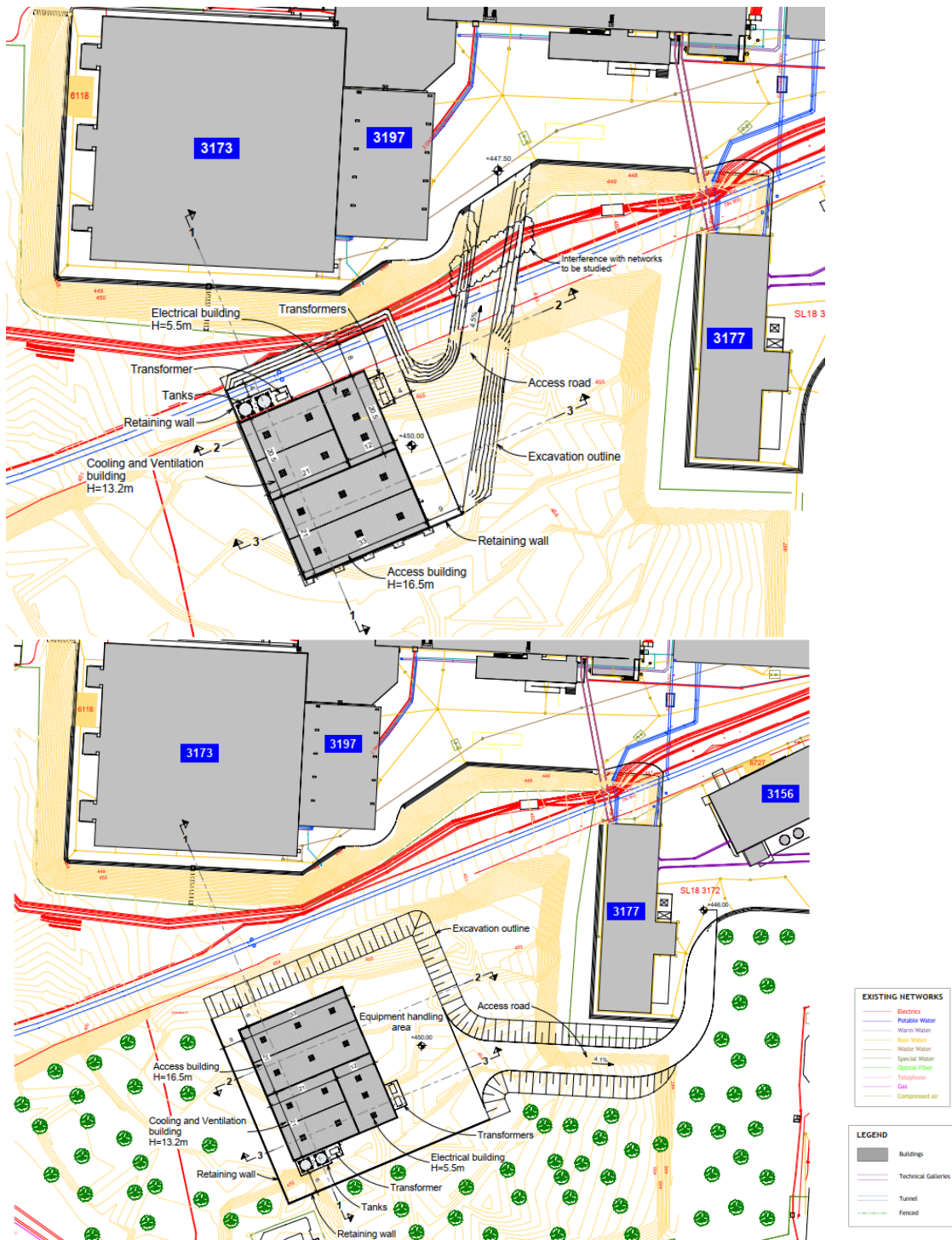


Figure 4: General layout of the proposed surface area. The top picture showing the initial design where the works interfere with the existing networks, the bottom picture showing the new design avoiding any interference.

### 3 Ventilation System

In Ref. [1] a rough estimate of the costing of the main FPF infrastructure and services was presented. The costing for the ventilation system was based on a crude extrapolation from the system used in the new HL-LHC underground infrastructure at point 1. Since this represented by far the largest cost for the infrastructure and services, a more detailed study of a possible ventilation system was carried out by the CERN cooling and ventilation group (EN-CV) in 2022.

The proposed preliminary design includes four separate systems:

- A dedicated smoke extraction system, based on three separate fire compartments;
- A liquid Argon (LAr) extraction system. This is needed due to the oxygen deficiency hazard posed by the large quantity of LAr in the FLArE detector;
- The pressurization system. This is needed to keep the safety corridor and part of the shaft pressurized and provide a safe escape route in case of fire and smoke;
- The normal ventilation system, which can extract 10,000 m<sup>3</sup>/hour.

A sketch of the preliminary design is shown in Figure 5, and the design and costing are described in more detail in Ref. [3].

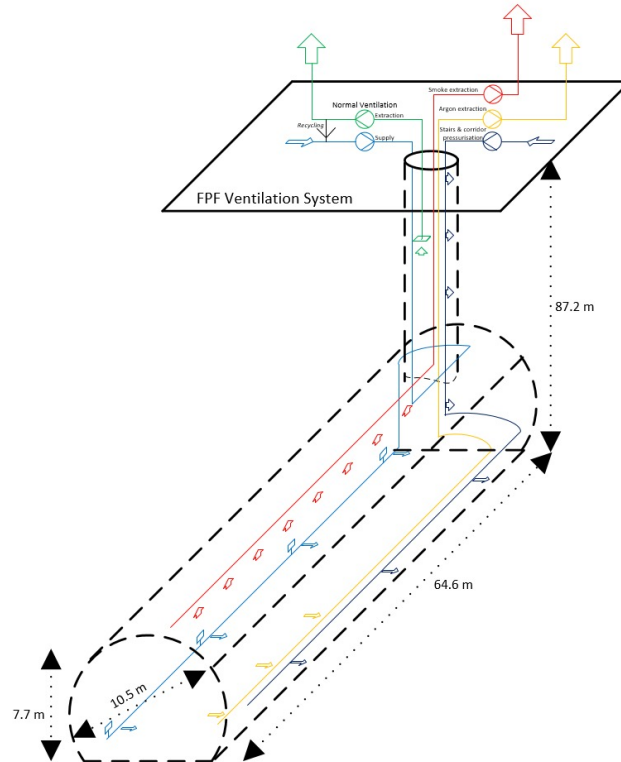


Figure 5: A sketch of the proposed FPF ventilation system design, showing the 4 independent systems.

This design assumes that the shaft is open to the air at the surface, which seems to be possible from initial discussion with the CERN Radio-protection team. It should be noted that the design will evolve as more information about the FPF experiments becomes available. In particular the requirements of the LAr extraction system will need to be revised once more details of the FLArE detector and its cryogenic system are finalized. The costing of this setup is estimated to be about 2.5 MCHF (including a 20% contingency), so substantially cheaper than the cost presented in Ref. [1].



## 4 Background particle rates at the FPF

In the Ref. [1], the aims of the FLUKA simulations regarding the FPF were presented. The first step was to provide a phase space of muons (the most abundant component of the detector background at the cavern) in an intermediate location that serves as source for further simulations to study the effect of a sweeper magnet and to optimize the CPU time required to obtain the muon fluence at the FPF.

### 4.1 Simulation technique

The goal of the FLUKA simulations was to estimate the muon fluence at the FPF cavern. Since the facility is located more than 600 m from the interaction point, the computational resources required to obtain meaningful statistics in a single step are too high in terms of time and number of cores. Therefore, a two step approach was adopted instead. In a first step, minimum bias proton-proton collisions at IP1 are directly simulated. Charged pion and kaon decay is then biased, associating to resulting muons a compensating statistical weight. Muons with a kinetic energy higher than 10 GeV are recorded when traversing a plane at 348.7 m from IP1. In fact, muons of lower energy will not reach the FPF due to the energy loss along the remaining path in the rock and the adoption of this threshold speeds up the calculations. In the second step, the recorded muons are loaded as source term and transported to the FPF with a 100 keV energy cutoff. Weight window biasing is implemented in order to limit statistical fluctuations (not all muons come from the aforementioned biased decay). This procedure is explained schematically in Figure 6.

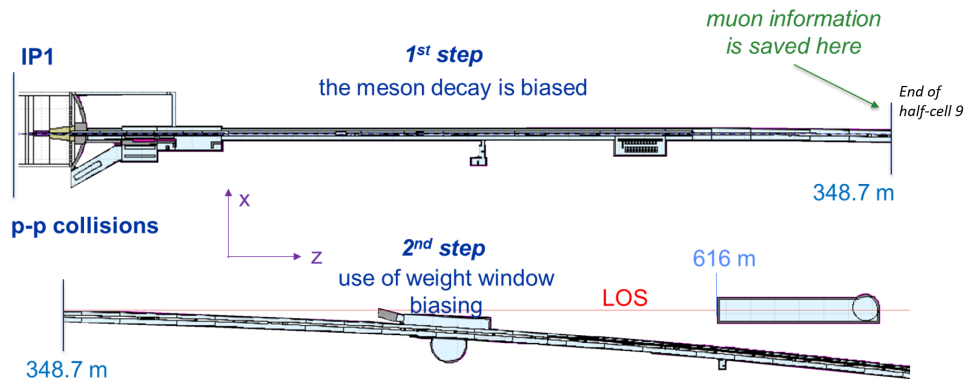


Figure 6: Scheme of the two steps simulation to assess the muon fluence in the FPF cavern.

### 4.2 Effect of full magnetic field maps of Long Straight Section magnets

In previous FLUKA calculations, full magnetic field maps, extending to the magnet yoke, were available only for a fraction of the elements in the relevant LHC portion. In particular,

the magnetic field region was limited to the two beam chambers in the case of the D2 separation dipole and the Q4 quadrupole, as shown in the bottom of Figure 7.

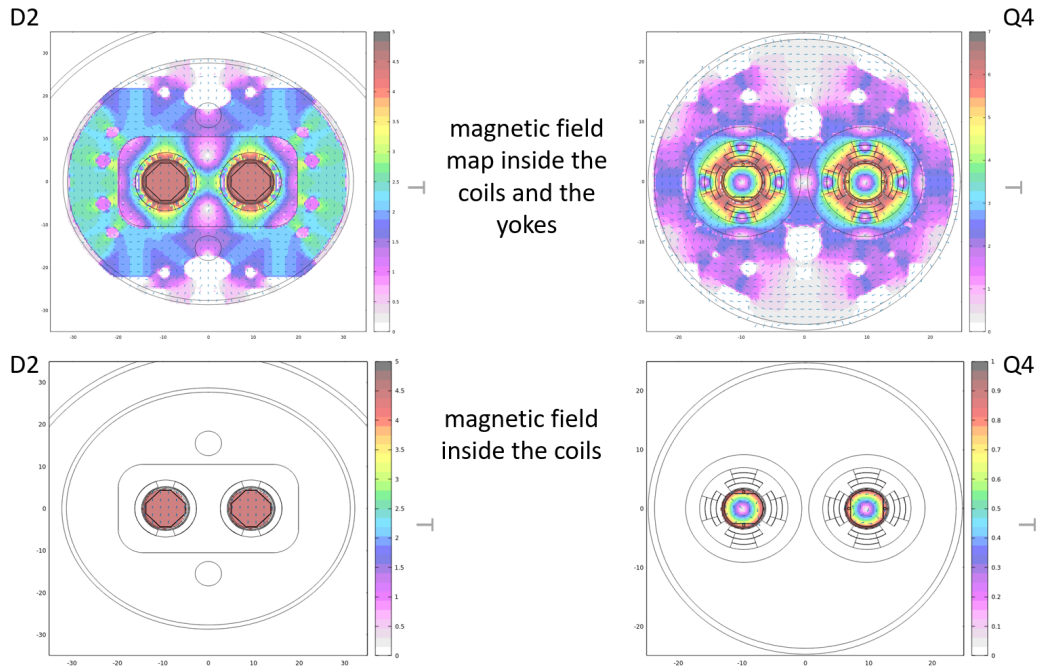


Figure 7: Magnetic field maps of the D2 recombination dipole (left) and Q4 matching section quadrupole (right). On the bottom it is shown the magnetic field in the two-bore region limited by the coils, as considered in previous simulations, while on the top the magnetic field region covers the whole magnet (courtesy of Susana Izquierdo Bermudez).

Thanks to the input of colleagues from the CERN magnet group, this inaccuracy has been now overcome (see the upper half of the same figure). As a result, the muon fluence rate along FPF turns out to be roughly halved, down to  $0.6 \text{ Hz/cm}^2$  at the HL-LHC nominal luminosity of  $5 \cdot 10^{34} \text{ cm}^{-2} \text{ s}^{-1}$  (referred to as  $5 L_0$  in this note). Positive muons account for one quarter of this value, while negative muons represent the remaining three quarters (i.e.,  $0.45 \text{ Hz/cm}^2$ ). The estimate is obtained by averaging over a  $20 \text{ cm}$  by  $20 \text{ cm}$  area centered on the ATLAS axis.

Figure 8 presents the spatial distribution of the positive and negative muon fluence rate in the horizontal plane, where the slope induced by the crossing angle can be appreciated.

### 4.3 Sweeper magnet potential

The installation of a sweeper magnet close to the LHC main magnets in the dispersion suppressor section at the end of the half-cell 10 (370 m from IP1) was considered to try to reduce the muon background in the FPF cavern.

The conceptual design of the sweeper magnet consists of a  $7 \text{ m}$  long square structure, with a  $10 \text{ cm}$  by  $10 \text{ cm}$   $\text{Sm}_2\text{Co}_{17}$  permanent magnet core surrounded by a  $20 \text{ cm}$  by  $20 \text{ cm}$

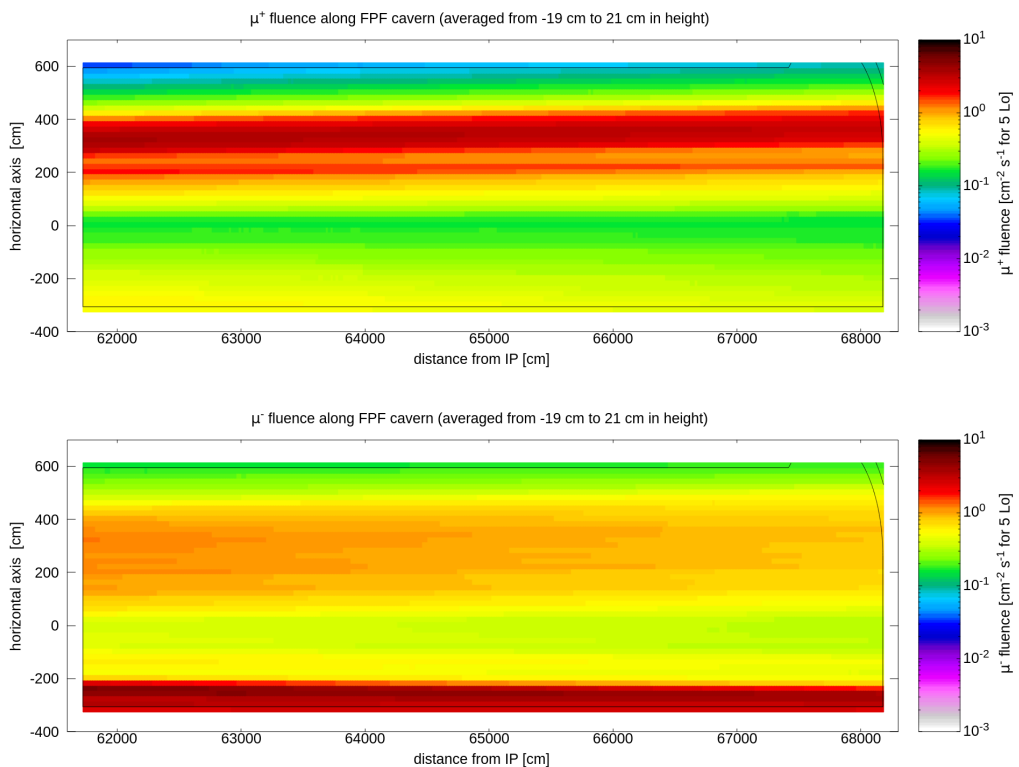


Figure 8: Spatial distribution of positive (top) and negative (bottom) muon fluence rate along the FPF cavern for  $5 L_0$  instantaneous luminosity. The 2D view is on the horizontal  $xz$  plane, with values averaged from  $-19$  cm to  $21$  cm in the missing vertical dimension, being  $y=0$  the beam height.

stainless steel frame. In Figure 9, its magnetic field map and position in the tunnel are shown. In the simulations, the magnet was displaced from the ATLAS axis ( $x=y=0$ ) to  $x = +9.2$  cm, in order to be aligned on the LOS that reflects the half crossing angle at the collision point, i.e.,  $250 \mu$  rad in the horizontal plane.

Different configurations for the sweeper magnet were explored, such as the rotation of the magnetic field, its displacement from  $x = 9.2$  cm to  $x = 55$  cm (at the location corresponding to the highest muon fluence in the FPF), and the enlargement of the magnet core of  $10$  cm by  $10$  cm to  $30$  cm by  $30$  cm and of the external frame to  $40$  cm by  $40$  cm (with the purpose of increasing the acceptance of the magnet).

The results from these studies are summarized in Table 1, where none of these configurations turn out to have a significant impact on the muon fluence rate at the FPF.

In the interpretation of these results, the scattering of muons in the rock may play a role. More than  $200$  m of rock are to be traversed between the point where muons exit the LHC tunnel, after the sweeper dipole, and the entrance of the FPF cavern. The muon trajectory deviations by Coulomb scattering re-populate the low fluence regions, as apparent in Figure 10. There one can appreciate that the artificial suppression of Coulomb scattering reduces the muon fluence rate in the region around the ATLAS axis at  $x=y=0$ , which in reality features higher values as long as Coulomb scattering is taken into account.

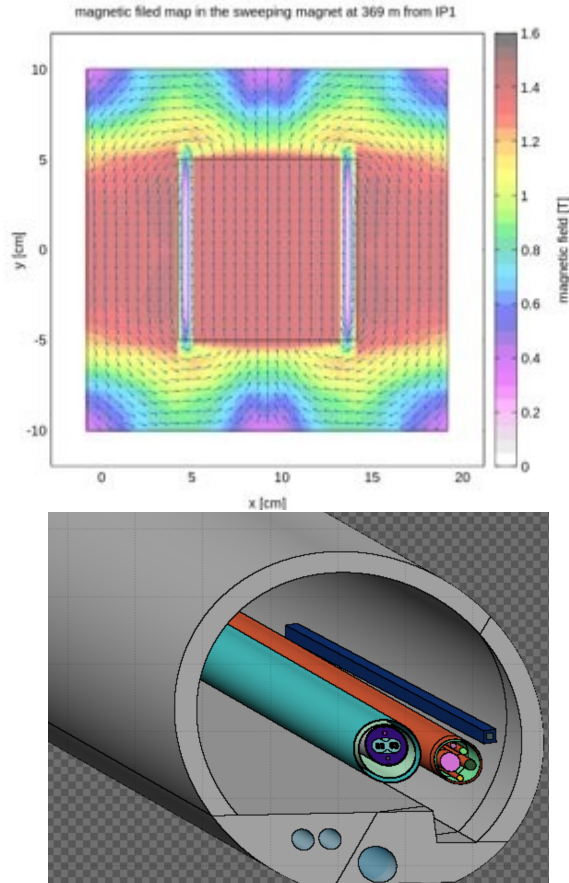


Figure 9: Top: Magnetic field map of the sweeper dipole. Bottom: Sweeper magnet (dark blue) in the LHC tunnel as implemented in the FLUKA geometry.

Configuration	$\Phi(\mu^+) \text{ cm}^{-2}\cdot\text{s}^{-1}$	$\Phi(\mu^-) \text{ cm}^{-2}\cdot\text{s}^{-1}$
Baseline: without sweeper magnet	0.15	0.45
Sweeper magnet centered at +9.2 cm with 10 cm by 10 cm section vertical-up magnetic field lines	0.17	0.45
Sweeper magnet centered at +55 cm with 10 cm by 10 cm section vertical/horizontal magnetic field lines	0.14-0.16	0.42-0.45
Sweeper magnet centered at +55 cm with 30 cm by 30 cm section vertical-down magnetic field lines	0.15	0.5

Table 1: Muon fluence rates on the ATLAS axis in the FPF cavern for different configurations of the sweeper magnet.

Despite these unsuccessful attempts, further investigations to see if different designs of a possible sweeper magnet could be effective will continue.

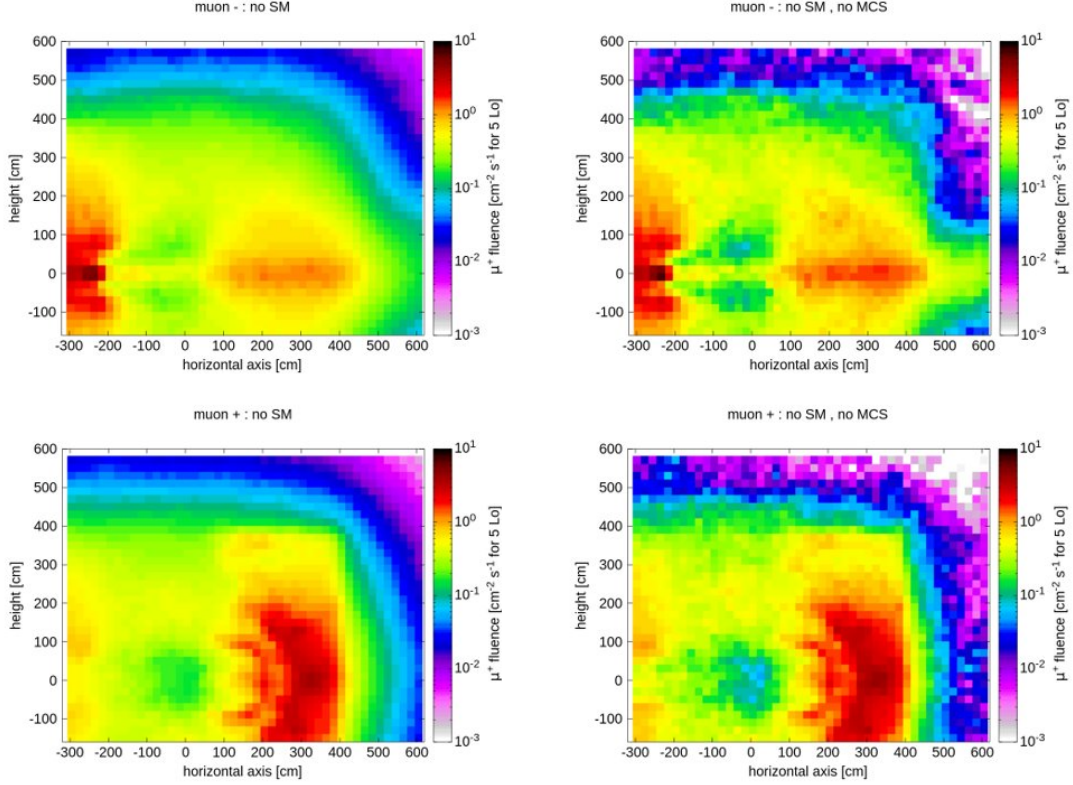


Figure 10: Transverse section xy view of the muon fluence rate in the FPF cavern, on the top for  $\mu^-$  and on the bottom for  $\mu^+$ , in the absence of sweeper magnet. In the right panels, Coulomb scattering was artificially disabled.

#### 4.4 First estimation of neutron field

Since the neutron fluence is an important input to the design of the FPF detectors and their electronics, its evaluation at the FPF was also performed, taking into account their generation in photonuclear interactions by both high energy photons and muons.

Figure 11 shows the neutron fluence rate spectrum, featuring its characteristic peaks, in particular the most prominent one on the left at thermal energies, and yielding an integral value approaching  $0.2 \text{ Hz/cm}^2$  at nominal HL-LHC luminosity (40% of which lies in the thermal peak).

In Figure 12, the transverse distributions of Silicon 1 MeV neutron equivalent fluence<sup>1</sup> and high energy hadron equivalent fluence at the entrance of the cavern are presented for an integrated luminosity corresponding to one year of ultimate HL-LHC operation. The annual high energy hadron equivalent fluence, determining the single event error rate in electronics, does not exceed  $3 \cdot 10^6 \text{ cm}^{-2} \text{ y}^{-1}$ , which is the threshold adopted in the LHC for declaring an area safe from the radiation to electronics (R2E) point of view [4].

<sup>1</sup>Virtual 1 MeV neutron fluence that produces the same damage in Silicon as the actual radiation field.

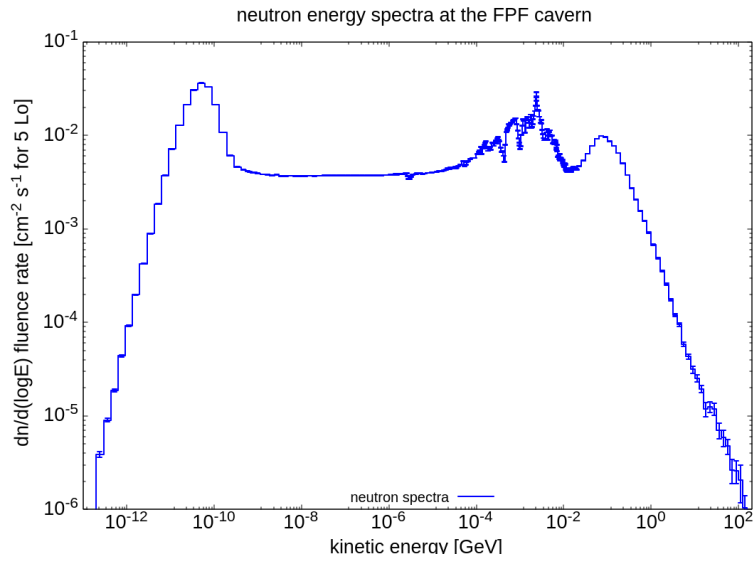


Figure 11: Neutron fluence rate spectrum in the FPF cavern for the nominal HL-LHC instantaneous luminosity.

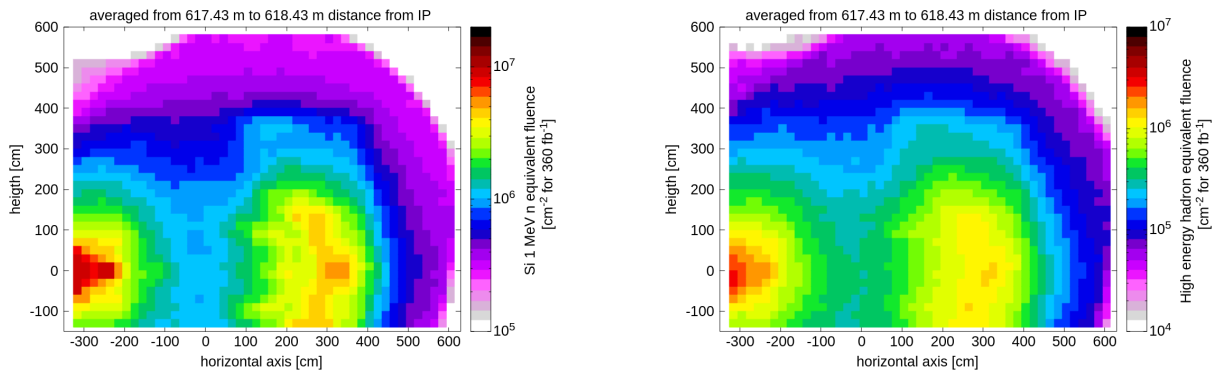


Figure 12: Silicon 1 MeV neutron equivalent fluence (top) and high energy hadron equivalent fluence (bottom) in the FPF cavern for  $360 \text{ fb}^{-1}$  integrated luminosity.

## 5 Radiation Protection studies

In the conception of new facilities, different Radiation Protection (RP) aspects need to be taken into account at the design level such as shielding requirements, radiation levels during operation (stray or prompt radiation) and technical stops (residual radiation), area classification, radiation monitoring, activation for future disposal of radioactive wastes, and more. Among them, the estimate of the stray radiation field is crucial for drafting the preliminary project proposal, identifying possible showstoppers and in general verifying that the preliminary plan complies with the CERN RP rules.

The CERN Radiation Protection rules are provided in the so-called "Safety Code F" [5, 6]. The objective of the Safety Code F is to define the rules for the protection of personnel, the population and the environment from ionising radiations produced at CERN. The Safety Code F is based and updated to the most advanced standards in the European and other relevant international legislation, including the legislation of CERN host states France and Switzerland.

The RP studies conducted in the context of the FPF project aim to:

- Determine the prompt radiation levels in the new experimental cavern and in the shaft for different scenarios (normal/abnormal LHC operation)
- Verify the accessibility of the experimental cavern/shaft during LHC and SPS operation.

These aspects are particularly relevant considering the requirement to access the new FPF cavern during HL-LHC operation. Areas inside CERN's perimeter are classified [7] as a function of the effective dose a person receives during their stay in the area under normal working conditions and routine operation. The potential external as well as internal exposures have to be taken into account when assessing the effective dose persons may receive when working in the area considered. The exposure limitation in terms of Effective Dose  $E$  is ensured by limiting correspondingly the operational quantity ambient dose equivalent rate  $\dot{H}^*(10)$  for exposure from external radiations. Action levels of specific airborne radioactive material (airborne radioactivity) and specific surface contamination at the corresponding workplaces for exposure from incorporated radionuclides are considered. In addition, exposure of people working on the CERN site, as well as the public, shall remain below the dose limits under normal as well as abnormal conditions of operation. Table 2 shows the limits for area classification of Non-designated and Supervised Radiation Areas at CERN: to allow access to the underground experimental area during LHC operation, the FPF cavern shall be classified with one of the levels of Table 2.

In the past years, the Radiation Protection group has provided a series of studies related to the conceptual design of the Forward Physics Facility [8, 9, 10, 11, 12]. The RP estimates are mainly based on FLUKA Monte Carlo simulations, making use of the model as described in Section 4. The model is indeed shared and maintained by a common effort and collaboration between SY-STI and HSE-RP CERN groups. The geometry has been updated following the suppression of the safety tunnel (Figure 13). With respect to the simulations reported in Section 4, the RP simulations considered different source terms (normal and abnormal operation) in order to estimate the stray radiation field relevant for the operation and accessibility of the FPF. In particular:

Area	Annual dose limit (year) $E$ [mSv]	Ambient dose equivalent rate (low-occupancy) $\dot{H}^*(10)$ [ $\mu$ Sv/h]
Non-designated	1	2.5
Supervised	6	15

Table 2: Relevant effective dose limits for area classification at CERN [7] for Non-Designated and Supervised Radiation Areas. Dose limits for Controlled Radiation Area not reported since not relevant for this study. FPF is considered a low-occupancy area, i.e.  $< 20\%$  working time.

- i **Beam-gas interactions.** This source term is relevant for the normal HL-LHC operation as it considers the inelastic interactions of the 7 TeV proton beam with residual gas within the beam pipes.
- ii **Loss of the HL-LHC beam.** Relevant for abnormal HL-LHC operation. This scenario takes into account the loss of the full HL-LHC 7 TeV proton beam on the MB.B15R1, i.e. the dipole that was located in front of the safety tunnel connection with the LHC tunnel in the initial design.
- iii **Loss of the SPS beam.** This source term is relevant for the access of the FPF shaft, as it considers the loss of the SPS 450 GeV proton beam in the closest location to the FPF infrastructure.
- iv **Direct muon component from IP1.** Relevant for normal operation conditions, this source term considers the muons directly streaming from ATLAS’s proton-proton collisions and from the particle showers produced in the Long Straight Section 1 (LSS 1) by the collision debris. This source term is based on the simulations reported in Section 4.

In all simulations, beam 1 (the clockwise beam beam leaving the right side of IP1) was simulated. The prompt ambient dose equivalent (rate) and the particle (neutrons, protons, charged pions, muons) spatial distribution was scored in the LHC tunnel, the safety tunnel (in preliminary studies) and the new experimental cavern by using Cartesian meshes. Finally, results have been normalized for ultimate HL-LHC operation conditions (corresponding to a luminosity of  $7.5 \times 10^{34} \text{ cm}^{-2}\text{s}^{-1}$ ).

A preliminary study released in 2021 [8] estimated the stray radiation field coming from the LHC, via the safety tunnel, due to beam-gas interactions (normal operational scenario), the full loss of the 7 TeV LHC proton beam on the MB.B15R1 magnet, which is the magnet closest to the connection to the FPF (abnormal operation scenario) and the loss of the SPS 450 GeV proton beam in the nearest location to the FPF access shaft (abnormal operation scenario). A summary of these estimates was presented at the 3<sup>rd</sup> FPF workshop [9]. Initially, the main constraint was identified in the radiation streaming through the safety tunnel, which translate in an Effective Dose higher than the limit for Supervised Radiation Area. The chicane within the safety tunnel was revised in a dedicated study [10]: a new 3 leg



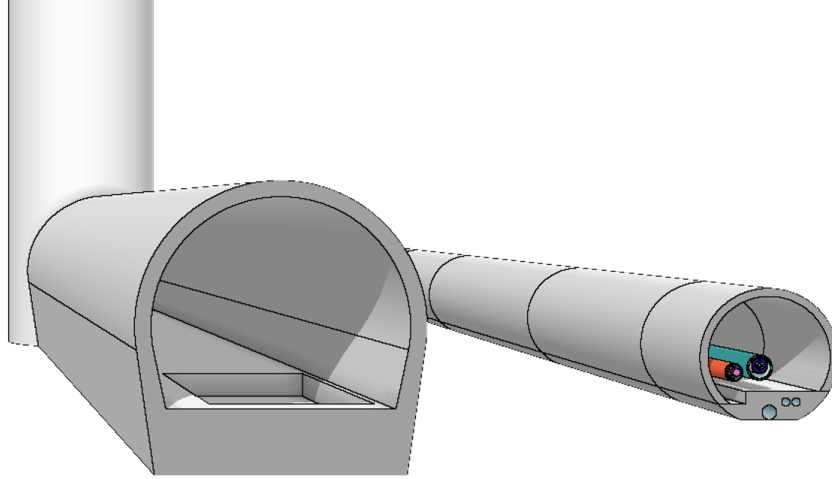


Figure 13: Geometry of the LHC tunnel and the FPF used in the FLUKA-RP simulation. The geometry has been updated following the suppression of the safety tunnel.

chicane, made of 80 cm thick walls, was implemented into the FLUKA model showing a beneficial impact in reducing the stray radiation field below the annual Effective Dose limit for Supervised Radiation Area. With the suppression of the safety tunnel, points *i* and *ii* become meaningless: indeed, without the connecting tunnel the streaming of radiation from the LHC to the FPF is sufficiently attenuated from the more than 10 m of rock separating the two facilities. Point *iii* remains still relevant, although negligible due to the distance (>35 m) between the SPS tunnel and the FPF shaft. Therefore, the main contribution to the stray radiation field comes from the muons streaming from IP1. A two-step simulation was performed by using the muon phase-space described in Section 4. The main outcome of this study has been reported in [11]. In addition, a HSE-RP Technical Note [12], summarizing all the RP estimates conducted in the context of the FPF project, is currently under finalization. The reader can refer to the latter report for more technical details and the complete set of results.

Figure 14 and Figure 15 show the 2D maps of the prompt ambient dose equivalent rate all along the FPF cavern as well as in three reference locations (IP-side of the cavern, middle of the cavern, non-IP side of the cavern). The simulations consider the full electromagnetic<sup>2</sup> (EM) transport, providing a more accurate estimate of the dose field. Figure 16 and Figure 17 show respectively the prompt ambient dose equivalent rate and the integrated ambient dose equivalent considering low (400 h) and permanent (2000 h) occupancy. In addition, Figure 16 and Figure 17 highlights the locations where the 1D profiles in Figure 18 and Figure 19 have been extracted.

The following considerations can be made from the RP estimates conducted for the FPF project:

- From studies in [8, 9, 10]:
  - Prompt dose rate from beam-gas interaction below  $2.5 \mu\text{Sv/h}$  (limit for non-

---

<sup>2</sup>I.e. transport of  $\gamma$ ,  $e^-$  and  $e^+$  down to specific energy thresholds set in the FLUKA input file.

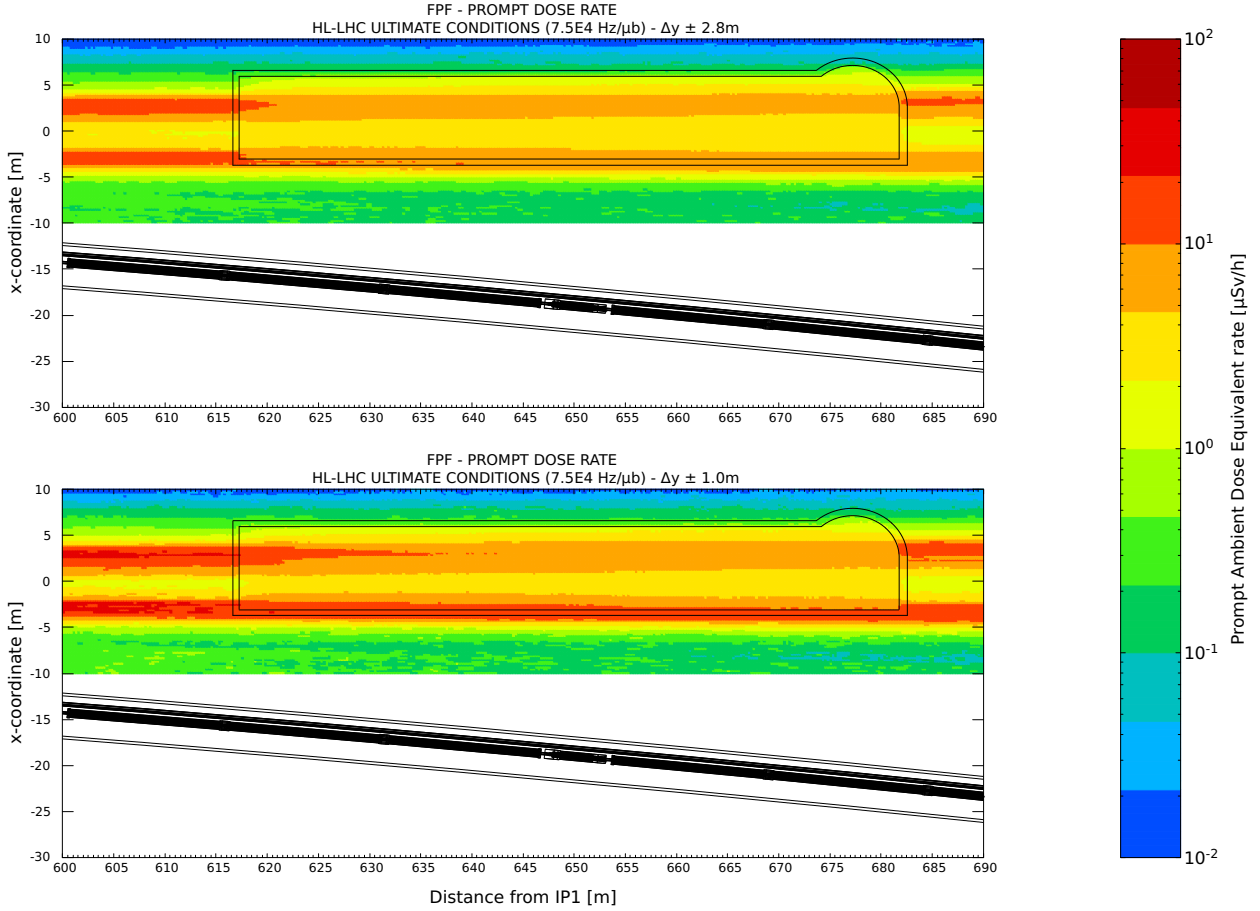


Figure 14: Prompt ambient dose equivalent rate,  $zx$ -plane (top view). Average over  $\Delta y = \pm 100$  cm.

designated areas);

- Dose from accidental LHC and SPS beam loss negligible due to suppression of the safety tunnel and distance from the FPF shaft;
- From studies in [11, 12]: Direct contribution from muons coming from IP1/LSS1 can limit the accessibility to the cavern during LHC operation, i.e.  $> 6$  mSv/year may be achieved locally;
- Classification of the cavern as Simple Controlled/Supervised Radiation Area (low-occupancy, i.e.  $< 20\%$  working time) seems possible;
- Access to the cavern during LHC beam operation will be limited to Radiation Workers<sup>3</sup>;

<sup>3</sup>Workers need to follow a dedicated RP training, depending on the exact area classification and the associated radiological risk. In addition, workers must wear, among other PPEs, personal passive/active dosimeter.

- No permanent control rooms are foreseen underground. During installation and commissioning there may be people in the cavern for an extended period: this time shall be quantified to finalize the RP risk assessment;
- Final study to be done considering a full integration model, i.e. including detectors, service equipment, and more;
- External personnel involved in the excavation (of the cavern and the lower part of the shaft) during beam operation have to be classified as “Radiation Workers”.

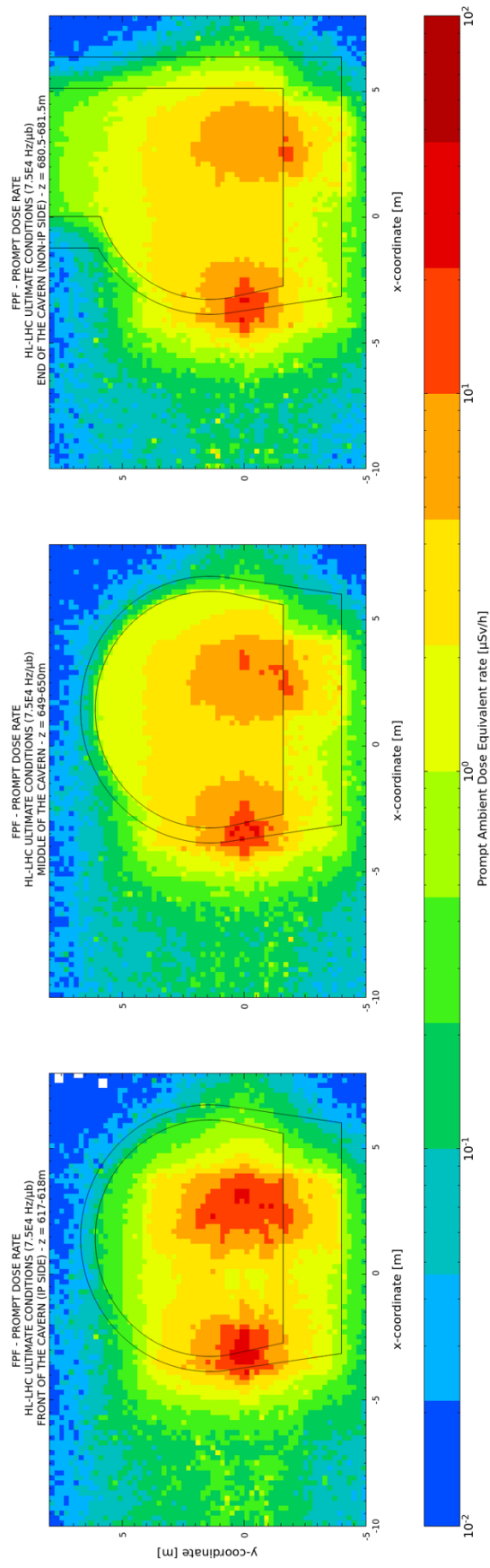


Figure 15: Prompt ambient dose equivalent rate,  $xy$ -plane (front view). Average over  $\Delta z = \pm 50$  cm.

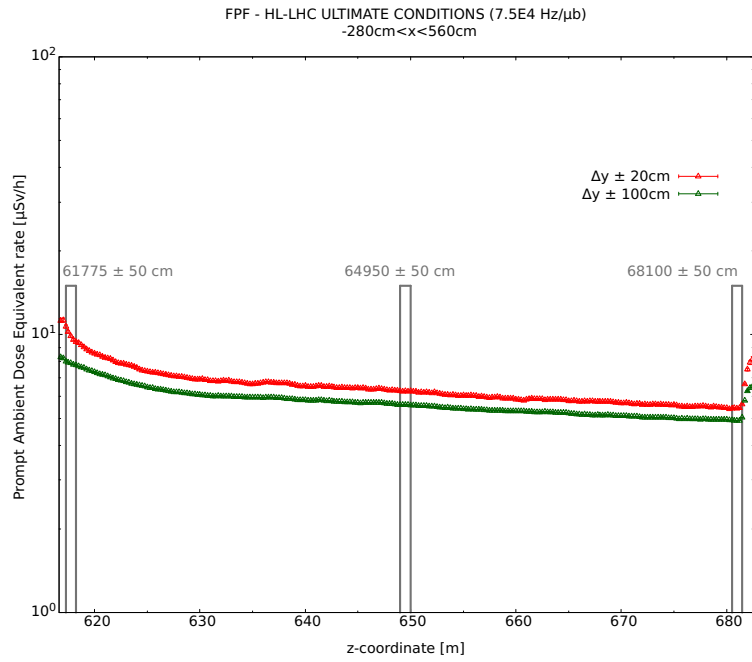


Figure 16: Prompt ambient dose equivalent rate,  $z$ -axis (longitudinal axis). Average over  $-280 < x < 560$  cm.

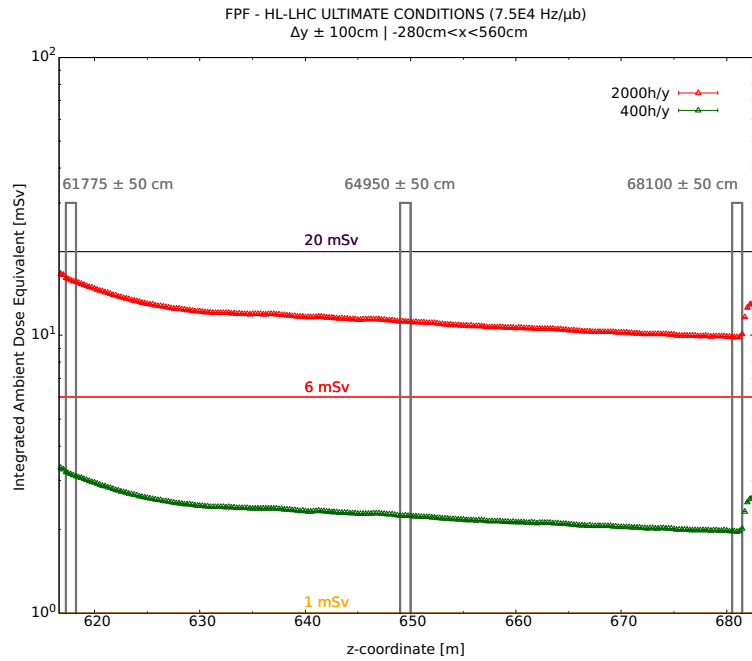


Figure 17: Integrated prompt ambient dose equivalent,  $z$ -axis (longitudinal axis), considering low (400 h) and permanent (2000 h) occupancy. Average over  $-280 < x < 560$  cm and  $\Delta y = \pm 100$  cm.

FPF - HL-LHC ULTIMATE CONDITIONS (7.5E4 Hz/ $\mu$ b)

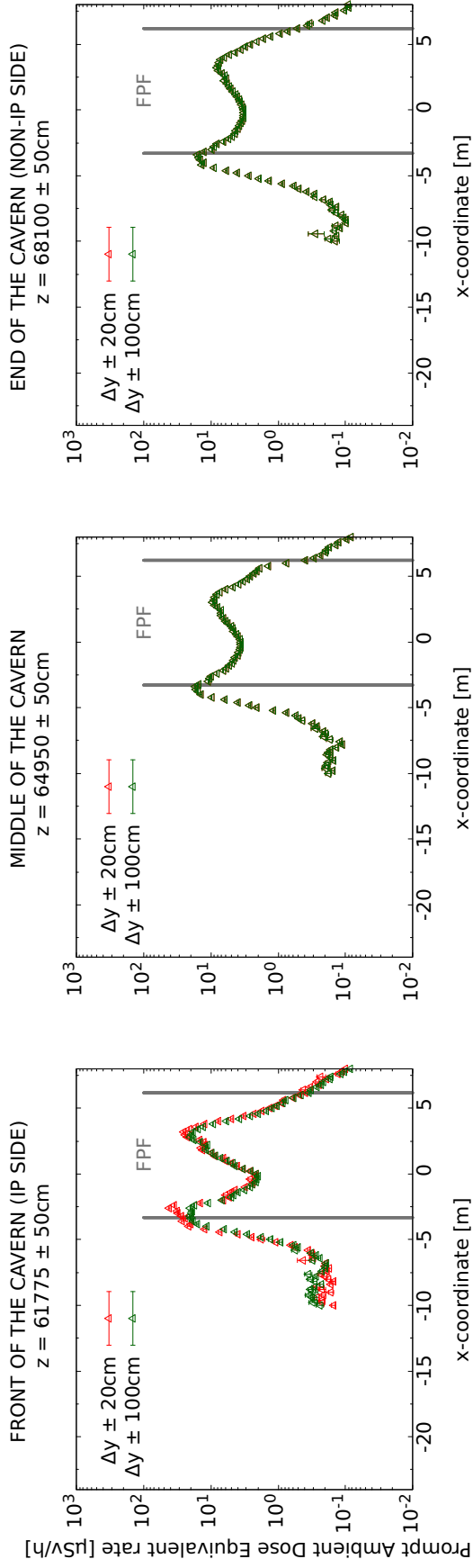


Figure 18: Prompt ambient dose equivalent rate,  $x$ -axis (transversal axis).

FPF - HL-LHC ULTIMATE CONDITIONS (7.5E4 Hz/ $\mu$ b) -  $\Delta y \pm 100$ cm

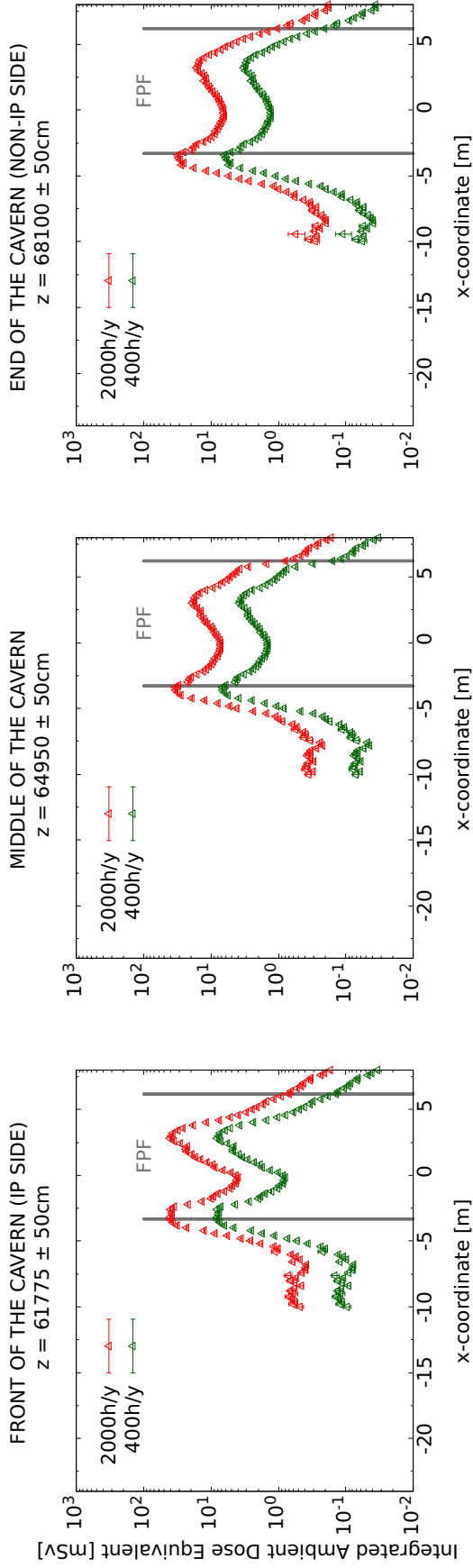


Figure 19: Integrated prompt ambient dose equivalent,  $x$ -axis (transversal axis), considering low (400 h) and permanent (2000 h) occupancy.

## 6 Summary

Progress on technical studies related to the implementation of the Forward Physics Facility design, as well as related to the inputs for the proposed experiments design has been described.

The connection gallery between the FPF and the LHC has been removed, and replaced by the creation of a safety corridor along the cavern. This minimizes the risks of damaging the LHC tunnel and opens the possibility of constructing the FPF cavern during machine operation, pending an ongoing analysis of the effects of vibration on LHC operation. In addition, the general layout of the surface area has been updated to avoid interfering with the existing technical networks. A preliminary design of the underground ventilation system has been provided leading to a significant cost reduction.

The muon background will constitute the main physics background to the FPF experiments. Estimates of this background using FLUKA simulations have been presented. These estimates take into account an improved modelling of the magnetic field in some of the LHC magnets, which reduces the overall muon fluence. The resulting background level is acceptable for the proposed FPF experiments. However, studies on a possible sweeping magnet show no significant reduction in the muon fluence. FLUKA simulation has also been used to estimate the neutron flux in the cavern, which shows that this is not expected to be a problem for the detectors or electronics.

Finally, the expected radiation level in the FPF cavern has been calculated. This study indicates that the main radiation hazard is posed by the muon flux, determining the classification of the area as Supervised Area with low occupancy. Access to the cavern during LHC operation will be limited to people trained as Radiation Workers. External personnel involved in the excavation of the cavern and the lower part of the shaft will similarly need to be classified as "Radiation workers".

## References

- [1] J. L. Feng *et al.*, "The Forward Physics Facility at the High-Luminosity LHC," *J. Phys. G*, vol. 50, no. 3, p. 030501, 2023.
- [2] "Physics Beyond Colliders Study Group," <https://pbc.web.cern.ch/>.
- [3] G. Peon, "Ventilation Installations for the Forward Physics Facility (FPF)," Tech. Rep. EDMS 2801032, 2022. [Online]. Available: <https://edms.cern.ch/document/2801032/1>
- [4] R. Garcia Alia, "Radiation safe level definition criteria for HL-LHC electronics," Tech. Rep. EDMS 2389056, 2021. [Online]. Available: <https://edms.cern.ch/document/2389056/1.1>
- [5] CERN, "Code F Rev. Radiation Protection - Radiation Protection Manual Radioprotection - Manuel de radioprotection," Tech. Rep. EDMS 335729, 2006. [Online]. Available: <https://edms.cern.ch/document/335729>



- [6] D. Forkel-Wirth, S. Roesler, M. Silari, M. Streit-Bianchi, C. Theis, H. Vincke, and H. Vincke, “Radiation protection at CERN,” Mar 2013, comments: 22 pages, contribution to the CAS - CERN Accelerator School: Course on High Power Hadron Machines; 24 May - 2 Jun 2011, Bilbao, Spain. [Online]. Available: <https://cds.cern.ch/record/1533023>
- [7] D. Forkel-Wirth, “Zonage radiologique au CERN,” Tech. Rep. EDMS 810149, 2007. [Online]. Available: <https://edms.cern.ch/document/810149/1>
- [8] L. Elie, A. Infantino, H. Vincke, “Preliminary RP considerations on the Forward Physics Facility (FPF) project,” Tech. Rep. EDMS 2632376, 2021. [Online]. Available: <https://edms.cern.ch/document/2632376/1>
- [9] A. Infantino, L. Elie, M. Maietta, H. Vincke, “Summary of the ongoing HSE-RP studies linked to the Forward Physics Facility,” Tech. Rep. EDMS 2645260, 2021. [Online]. Available: <https://edms.cern.ch/document/2645260/1>
- [10] L. Elie, A. Infantino, H. Vincke, “Updated RP studies on the FPF chicane,” Tech. Rep. EDMS 2717012, 2022. [Online]. Available: <https://edms.cern.ch/document/2717012/1>
- [11] A. Infantino, L. Elie, H. Vincke, “Radiation Protection studies for the Forward Physics Facility project: prompt muon dose,” Tech. Rep. EDMS 2797521, 2022. [Online]. Available: <https://edms.cern.ch/document/2797521/1>
- [12] L. Elie, A. Infantino, H. Vincke, “Radiation protection studies for the Forward Physics Facility,” Tech. Rep. EDMS 2771345, 2022. [Online]. Available: <https://edms.cern.ch/document/2771345/1>